Properties of superconductivity on a density wave background with small ungapped Fermi surface parts

P. D. Grigoriev*
L. D. Landau Institute for Theoretical Physics, 142432 Chernogolovka, Russia
(Received 19 February 2008; revised manuscript received 20 May 2008; published 18 June 2008)

We investigate the properties and the microscopic structure of superconductivity (SC) coexisting and sharing the common conducting band with density wave (DW). Such coexistence may take place when the nesting of the Fermi surface (FS) is not perfect, and in the DW state some quasiparticle states remain on the Fermi level and lead to the Cooper instability. The dispersion of such quasiparticle states strongly differs from that without DW, and so do the properties of SC on the DW background. The upper critical field H_{c2} in such a SC state increases as the system approaches the critical pressure, where the ungapped quasiparticles and superconductivity just appear, and it may considerably exceed the usual H_{c2} value without DW. The spin-density wave (SDW) background strongly suppresses the singlet SC pairing, while it does not affect so much the triplet SC transition temperature. The results obtained explain the experimental observations in layered organic metals $(TMTSF)_2PF_6$ and α-$(BEDT\text{-}TTF)_2KHg(SCN)_4$, where SC appears in the DW states under pressure and shows many unusual properties.

DOI: 10.1103/PhysRevB.77.224508 PACS number(s): 74.70.Kn, 71.30.+h

I. INTRODUCTION

The interplay between superconductivity (SC) and insulating charge or spin-density wave states is a subject of an active investigation for more than 30 years (for a review see, e.g., Ref. 1). The density wave (DW) is traditionally considered as a strong obstacle for the formation of SC, as it creates an energy gap at the Fermi level.[2–4] The coexistence of DW and SC has been considered in metals with several conducting bands or with imperfect nesting, when even in the DW state there is a finite electron density on the Fermi level.[5–7] Then the transition temperature T_c^{SC} to the SC state reduces exponentially when the DW is formed, because the electrons participating in the formation of DW drop out from the SC condensate.[5,6]

However, in several compounds [e.g., in layered organic superconductors $(TMTSF)_2PF_6$ and α-$(BEDT\text{-}TTF)_2KHg(SCN)_4$],[8,9] the SC transition temperature on the DW background is very close to (or even exceeds) T_c^{SC} without DW. In $(TMTSF)_2PF_6$ superconductivity coexists with spin-density wave (SDW) state at temperature below $T_c^{SC} \approx 1.1$ K in the pressure interval above some critical pressure $P_{c1} \approx 8.5$ kbar, but below $P_c \approx 9.5$ kbar, at which the SDW phase undergoes the first-order phase transition into the metallic state (see Fig. 7 of Ref. 8 and the schematic phase diagram in Fig. 1). This coexistence is even more surprising, as this compound has only one quasi-one-dimensional (1D) conducting band. Special attention was given to the fact that the upper critical field H_{c2} in this superconducting state exceeds several times the expected paramagnetic limit[10] (see Refs. 11 and 12), and no change in the Knight shift has been observed in this compound as the temperature lowers to this SC state.[13] Both these features suggest the spin-triplet superconducting paring in $(TMTSF)_2PF_6$. In addition, the upper critical field H_{c2} perpendicular to the conducting layers strongly increases as the pressure approaches P_{c1} and has an unusual upward curvature as a function of temperature,[14] suggesting that the SDW has a very strong influence on the SC properties of this phase. The electronic structure of this mixed phase is still under debate. A phase separation in the form of macroscopic metallic and DW domains,[8,14] being natural with the constant volume constraint, seems strange at fixed pressure, when the whole sample may choose the state with the lowest free energy. The pressure and temperature dependence of the upper critical field requires[14] that the size d of the SC domains, if they exist, must be much less than the SC coherence length $\xi_{SC} \sim 10^{-4}$ cm as the pressure approaches P_{c1} [see Eq. (59) and the discussion in Sec. III]. This raises many questions about the structure of such a mixed state, because if the domain width is comparable to the SDW coherence length, this confinement of the electron wave functions costs additional energy greater than the SC energy gap. The angular magnetore-

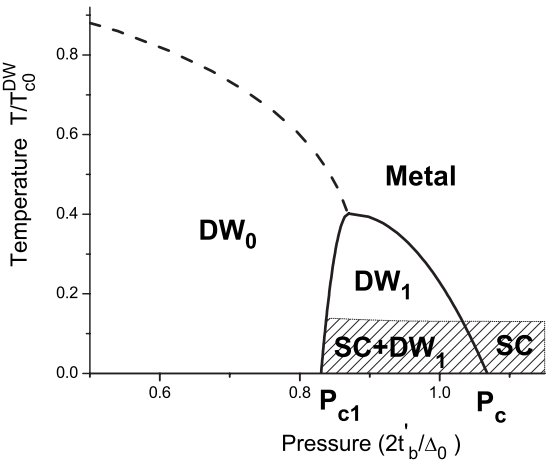

FIG. 1. The schematic picture of the phase diagram in $(TMTSF)_2PF_6$, where superconductivity coexists with DW in some pressure interval above P_{c1} but below P_c. DW_0 stands for the uniform fully gapped DW. DW_1 denotes the DW state when the imperfect nesting term t_b' is strong enough as compared to the SDW energy gap Δ_0, so that the ungapped FS pockets or nonuniform DW structure appear.

sistance oscillations[15] do not give a definite test on whether the spatial phase separation occurs on a scale greater than the SC coherence length.

An alternative to the picture[8,14] of macroscopic DW and normal (or SC) domains in $(TMTSF)_2PF_6$ has been proposed recently.[16,17] According to Ref. 17, there are two different structures where SC coexists microscopically with DW. In the first structure, the destruction of the insulating DW phase at $P>P_{c1}$ goes via forming the ungapped metallic pockets in the electronic spectrum, which spread over the momentum space, merging into the normal metallic state gradually or via a phase transition. This scenario, analogous to the one studied in Refs. 5 and 6, however, differs from it, since the formation of DW strongly modifies the quasiparticle dispersion in the ungapped parts of the Fermi surface, changing the properties of SC state on the DW background. In the second scenario, the DW order parameter at pressure $P>P_{c1}$ becomes spatially nonuniform by means of amplitude solitons. These soliton structures are familiar in charge-density wave (CDW) states at high pressure or in magnetic field (see, e.g., the reviews in Refs. 18 and 19). The normal or SC phase appears first as metallic domain walls, and the concentration of these soliton walls increases with increasing pressure. At finite density of solitons, i.e., above P_{c1}, the electron wave functions of single solitons strongly overlap, forming a new periodic conducting metallic network on the DW background. If it were not for the first-order transition with the further increase in soliton density, the new phase is expected to merge gradually into the metallic state.

Both microscopic structures may appear in DW superconductors. Nuclear-magnetic-resonance (NMR) experiments[20] are consistent with the scenario where the phase separation takes place on the microscopic scale not exceeding the DW coherence length, thus supporting either of the above scenarios. In both scenarios, at low enough temperature, superconductivity appears at pressure $P>P_{c1}$,[17] and the DW have a strong influence on the properties of such a mixed SC state.[21] The SDW background strongly reduces the spin-singlet SC transition temperature, making the spin-triplet pairing more favorable,[17] in agreement with experiments on $(TMTSF)_2PF_6$.[11–13] This feature appears due to the spin-dependent scattering on the SDW condensate, and it does not happen when superconductivity coexists with CDW. However, the CDW background modifies the quasiparticle spectrum and renormalizes the e-e interaction, which also changes the SC properties.

In the present paper we follow the ideas in Ref. 17 and study in detail the microscopic structure and properties of the mixed SC-DW state in the first scenario of uniform DW with ungapped metallic pockets above $P>P_{c1}$. We show that the modification of the quasiparticle spectrum by the DW background strongly changes many SC properties, such as the pressure dependence of the upper critical field. In Sec. II we generalize the model in Ref. 17 to the case of a more realistic e-e interaction with backward and forward scattering, and describe in detail the uniform DW state with ungapped pockets. In Sec. III we estimate the SC transition temperature and the upper critical field H_{c2} in the DW-SC mixed state, and show that H_{c2} strongly increases as the pressure approaches the critical value P_{c1}, in agreement with experiments on $(TMTSF)_2PF_6$ and α-$(BEDT\text{-}TTF)_2KHg(SCN)_4$. In Sec. IV we study SC on SDW background and show that SDW strongly suppresses only the spin-singlet SC ordering, thus favoring the triplet SC state. Our results are aimed mainly at quasi-1D metals, but can also be applied to other DW superconductors with slightly imperfect nesting.

II. MODEL AND DENSITY WAVE STATE WITHOUT SUPERCONDUCTIVITY

A. Model

In quasi-1D metals the free-electron dispersion without magnetic field is written down as

$$\varepsilon(\boldsymbol{k}) = \pm v_F(k_x \mp k_F) + t_\perp(\mathbf{k}_\perp). \tag{1}$$

The electron dispersion in the easy-conducting (chain) x direction is strong and can be linearized near the Fermi surface (FS). The interchain dispersion $t_\perp(\boldsymbol{k}_\perp)$ is much weaker and given by the tight-binding model with few leading terms,

$$t_\perp(\boldsymbol{k}_\perp) = 2t_b \cos(k_y b) + 2t'_b \cos(2k_y b) + 2t_c \cos(k_z \tilde{c}), \tag{2}$$

where $b, \tilde{c}$ are the lattice constants in the y and z directions. The dispersion along the z axis is considerably weaker than that along the y direction and does not play any role in the analysis below. The FS consists of two warped sheets and possesses an approximate nesting property, $\varepsilon(\boldsymbol{k}) \approx -\varepsilon(\boldsymbol{k}-\boldsymbol{Q})$, which leads to the formation of DW at low temperature. The nesting property is spoiled only by the second term $t'_b(k_y)$ in Eq. (2), which, therefore, is called the "antinesting" term. Increase in the latter with applied pressure leads to the transition in the gapped DW state at $P=P_{c1}$, where the ungapped pockets on the FS or isolated soliton walls[22] first appear. In the pressure interval $P_{c1}<P<P_c$, the new state develops, where the DW coexists with superconductivity at rather low temperature $T<T_c^{SC}$, while at high temperature $T>T_{SC}$ the DW state coexists with the metallic phase.

The electron Hamiltonian is

$$\hat{H} = \hat{H}_0 + \hat{H}_{\text{int}}, \tag{3}$$

with the free-electron part in momentum representation

$$\hat{H}_0 = \sum_{\boldsymbol{k}} \varepsilon(\boldsymbol{k}) a^\dagger_\alpha(\boldsymbol{k}) a_\alpha(\boldsymbol{k}) \tag{4}$$

and the interaction part

$$\hat{H}_{\text{int}} = \frac{1}{2} \sum_{\boldsymbol{k}\boldsymbol{k}'\boldsymbol{Q}} V_{\alpha\beta\gamma\delta}(\boldsymbol{Q}) a^\dagger_\alpha(\boldsymbol{k}+\boldsymbol{Q}) a_\beta(\boldsymbol{k}) \times a^\dagger_\gamma(\boldsymbol{k}'-\boldsymbol{Q}) a_\delta(\boldsymbol{k}'). \tag{5}$$

Here and below we imply the summation over repeating spin indices. The interaction potential is

$$V_{\alpha\beta\gamma\delta}(\boldsymbol{Q}) = U_c(\boldsymbol{Q}) I_{\alpha\beta} I_{\gamma\delta} - U_s(\boldsymbol{Q}) \vec{\sigma}_{\alpha\beta} \vec{\sigma}_{\gamma\delta}, \tag{6}$$

where $\vec{\sigma}_{\alpha\beta}$ are the Pauli matrices, $I_{\alpha\beta}$ is the 2×2 unity matrix. For the formation of DW, only the value of this potential at the nesting vector $\boldsymbol{Q}=\boldsymbol{Q}_N$ is important. The values $U_c(\boldsymbol{Q}_N)$

and $U_s(\boldsymbol{Q}_N)$ are called the charge and spin coupling constants. Depending on their ratio, the charge- or spin-density wave is formed.

For superconducting pairing, both the momentum and the frequency dependences of potential (6) are important. Below we consider only a simplified model, similar to the BCS model,[23] where the frequency dependence of the interaction potential is taken into account only through the ultraviolet cutoff (Debye frequency) in the Cooper loop. The phonon-mediated e-e interaction is always attractive and contributes only to the spin-independent charge coupling $U_c(\boldsymbol{Q})$. The Coulomb and the exchange e-e interaction produce both the charge $U_c(\boldsymbol{Q})$ and the spin $U_s(\boldsymbol{Q})$ couplings.

Without DW, the coupling functions $U_c(\boldsymbol{Q})$ and $U_s(\boldsymbol{Q})$ determine the possibility and the type of SC pairing (for a review, see Refs. 24–26). In the presence of DW instability, the bare couplings $U_{c0}(\boldsymbol{Q})$ and $U_{s0}(\boldsymbol{Q})$ may be strongly renormalized, which affects the type and the transition temperature of SC.[25,26] Many theoretical approaches have been used to calculate the effective SC interaction in the presence of DW instability: the summation of ladder diagrams in 1D metals,[27] the random-phase approximation (RPA) in quasi-1D metals,[28,29] the renormalization-group approach,[30,31] the perturbation theory up to the third order,[32] fluctuation-exchange method,[33] etc. The renormalized functions $U_c(\boldsymbol{Q})$ and $U_s(\boldsymbol{Q})$ depend strongly on the bare couplings,[28,30] which are, usually, unknown. Therefore, the theoretical predictions about the type of SC pairing in the particular compounds are still uncertain and often contradictory.

In addition to the renormalization of the e-e interaction, the DW affects strongly the quasiparticle energy spectrum. This change in the quasiparticle energy spectrum leads to the qualitatively new SC properties, such as the strong pressure dependence of the upper critical field H_{c2}. Even when neglecting the renormalization of the e-e interaction, the SDW background strongly affects the type of SC paring.[17] To focus on the influence of the new quasiparticle spectrum on the SC properties on the DW background, we use the simplified model of the e-e interaction and set $U_s(\boldsymbol{Q})=0$. Inclusion of $U_s(\boldsymbol{Q})\neq 0$ changes only the SC coupling constants for various types of pairing [see Eq. (10) of Ref. 25]. Many essential qualitative features of SC on the DW background, such as the increase in the upper critical field and the suppression of singlet SC by the SDW background, can be obtained in this simplified model. Concerning the momentum dependence of $U_c(\boldsymbol{Q})$, in 1D and quasi-1D metals one, usually, distinguishes only the backward and forward scattering:

$$U_c(\boldsymbol{Q}) = \begin{cases} U_c^f, & Q_x \ll 2k_F \\ U_c^b, & Q_x \approx 2k_F. \end{cases} \tag{7}$$

Depending on the signs and the ratio of backward U_c^b and forward U_c^f coupling constants, one has a singlet or a triplet SC pairing. Strong Q_y dependence of the e-e interaction may lead to the d- and f-wave SC pairings.[30,31] We do not consider these exotic SC pairings, due to the absence of their experimental evidence in quasi-1D organic metals. The available thermal conductivity measurements in organic DW superconductors show the nodeless SC order parameter,[34] which excludes most higher-harmonic pairings. Hamiltonian (3) does not also include the spin-orbit interaction, which is assumed to be weak.

Below we take the DW transition temperature to be much greater than the SC transition temperature, $T_c^{\mathrm{DW}} \gg T_c^{\mathrm{SC}}$, which corresponds to most DW superconductors. For example, in $(\mathrm{TMTSF})_2\mathrm{PF}_6$, $T_c^{\mathrm{SDW}} \approx 8.5\ \mathrm{K} \gg T_c^{\mathrm{SC}} \approx 1.1\ \mathrm{K}$ and in α-$(\mathrm{BEDT\text{-}TTF})_2\mathrm{KHg(SCN)}_4$, $T_c^{\mathrm{CDW}} \approx 8\ \mathrm{K} \gg T_c^{\mathrm{SC}} \approx 0.1\ \mathrm{K}$. Therefore, we first study the structure of the DW state in the pressure interval $P_{c1} < P < P_c$, and then consider the superconductivity on this background.

B. Uniform density wave state with ungapped states

In the case of the uniform DW order parameter, $\Delta_0(x) = \Delta_0 = \mathrm{const}(T,P)$, the electron Green's functions in the DW state in the mean-field approximation can be written down explicitly. We introduce the thermodynamic Green's function

$$\hat{g}_{\alpha\beta}(\boldsymbol{k}',\boldsymbol{k},\tau-\tau') = \langle T_\tau \{ a_\alpha^\dagger(\boldsymbol{k}',\tau') a_\beta(\boldsymbol{k},\tau) \} \rangle, \tag{8}$$

where the operators are taken in the Heisenberg representation and Green's function $\hat{g}_{\alpha\beta}(\boldsymbol{k}',\boldsymbol{k},\tau-\tau')$ is an operator in the spin space. The CDW order parameter

$$\hat{\Delta}_{\boldsymbol{Q}} = U_c \sum_{\boldsymbol{k}} \hat{g}(\boldsymbol{k}-\boldsymbol{Q},\boldsymbol{k},-0) = \Delta_{\boldsymbol{Q}} \tag{9}$$

is a unity operator in spin space, and the SDW order parameter is

$$\hat{\Delta}_{\boldsymbol{Q}\alpha\beta} = U_s(\vec{\sigma}_{\alpha\beta}\cdot\vec{\sigma}_{\gamma\delta}) \sum_{\boldsymbol{k}} \hat{g}_{\gamma\delta}(\boldsymbol{k}-\boldsymbol{Q},\boldsymbol{k},-0) = (\vec{\sigma}\vec{l})\Delta_{\boldsymbol{Q}}, \tag{10}$$

where the complex vector $\vec{l}$ determines the polarization of the SDW. In the presence of magnetic field $\vec{H}$ and without internal magnetic anisotropy, $\vec{l} \perp \vec{H}$. Below, the external magnetic field is taken to be rather weak, affecting only SC but not the DW,[35] because a strong magnetic field would suppress SC. We consider only one DW order parameter, i.e., $\Delta_{\boldsymbol{Q}} \neq 0$ only for $\boldsymbol{Q} = \pm \boldsymbol{Q}_N$, where $\boldsymbol{Q}_N \approx 2k_F\boldsymbol{e}_x + (\pi/b)\boldsymbol{e}_y + (\pi/\tilde{c})\boldsymbol{e}_z$, and $\boldsymbol{e}_x, \boldsymbol{e}_y, \boldsymbol{e}_z$ are the unit vectors in the x,y,z directions. In the mean-field approximation, one has

$$\hat{H}_{\mathrm{int}} = \frac{1}{2} \sum_{\boldsymbol{Q}\boldsymbol{k}} a_\alpha^\dagger(\boldsymbol{k}+\boldsymbol{Q}) a_\beta(\boldsymbol{k}) \hat{\Delta}_{\boldsymbol{Q}\alpha\beta}.$$

The hermicity of the Hamiltonian requires $\hat{\Delta}_{-\boldsymbol{Q}\alpha\beta} = \hat{\Delta}^*_{\boldsymbol{Q}\beta\alpha}$. Below we omit the explicit spin indices, keeping only the "hat" symbol above the spin operators. For SDW the equations of motion in the frequency representation are

$$[i\omega - \varepsilon(\mathbf{k})]\hat{g}(\boldsymbol{k}',\boldsymbol{k},\omega) - \sum_{\boldsymbol{Q}} \Delta_0(\vec{\sigma}\vec{l})\hat{g}(\boldsymbol{k}',\boldsymbol{k}-\boldsymbol{Q},\omega) = \delta_{\boldsymbol{k}'\boldsymbol{k}}. \tag{11}$$

If we neglect the scattering into the states with $|k_x| \gtrsim 2k_F$, the equations of motion (11) decouple,

$$\begin{pmatrix} i\omega_n - \varepsilon(\mathbf{k}) & \Delta_0(\vec{\sigma}\vec{l}) \\ \Delta_0^*(\vec{\sigma}\vec{l}) & i\omega_n - \varepsilon(\mathbf{k}-\mathbf{Q}) \end{pmatrix} \hat{G} = \hat{I}, \tag{12}$$

where the matrix Green's function

$$\hat{G} \equiv \begin{pmatrix} g^{RR}(\mathbf{k},\mathbf{k},\omega) & g^{LR}(\mathbf{k}-\mathbf{Q},\mathbf{k},\omega)(\vec{\sigma}\vec{l}) \\ g^{RL}(\mathbf{k},\mathbf{k}-\mathbf{Q},\omega)(\vec{\sigma}\vec{l}) & g^{LL}(\mathbf{k}-\mathbf{Q},\mathbf{k}-\mathbf{Q},\omega) \end{pmatrix}, \tag{13}$$

$\hat{I}$ is the 2×2 identity matrix, and the R and L superscripts denote the right and left FS sheet of electrons,

$$a_\alpha(\mathbf{k},\tau) \equiv \begin{cases} a_\alpha^R(\mathbf{k},\tau), & k_x > 0 \\ a_\alpha^L(\mathbf{k},\tau), & k_x < 0. \end{cases} \tag{14}$$

The electron Green's functions in the CDW state are obtained from Eqs. (12) and (13) by removing the spin factor $(\vec{\sigma}\vec{l})$ from the nondiagonal elements.

Introducing the notations

$$\varepsilon_\pm(\mathbf{k}',\mathbf{k}) = [\varepsilon(\mathbf{k}') \pm \varepsilon(\mathbf{k})]/2 \tag{15}$$

and

$$E_{1,2}(\mathbf{k}) \equiv \varepsilon_+(\mathbf{k},\mathbf{k}-\mathbf{Q}) \pm \sqrt{\varepsilon_-^2(\mathbf{k},\mathbf{k}-\mathbf{Q}) + |\Delta_0|^2}, \tag{16}$$

from Eq. (12) one has

$$g^{LR}(\mathbf{k}-\mathbf{Q},\mathbf{k},\omega) = \frac{\Delta_0}{[i\omega - E_1(\mathbf{k})][i\omega - E_2(\mathbf{k})]},$$

$$g^{RL}(\mathbf{k},\mathbf{k}-\mathbf{Q},\omega) = \frac{\Delta_0^*}{[i\omega - E_1(\mathbf{k})][i\omega - E_2(\mathbf{k})]}, \tag{17}$$

and

$$g^{RR}(\mathbf{k},\mathbf{k},\omega) = \frac{i\omega - \varepsilon(\mathbf{k})}{[i\omega - E_1(\mathbf{k})][i\omega - E_2(\mathbf{k})]} = g^{LL}(\mathbf{k},\mathbf{k},\omega). \tag{18}$$

The ungapped pockets on the Fermi surface with energy spectrum (16) appear when $|\varepsilon_+(\mathbf{k})|_{\max} = 2t'_b > |\Delta_0|$, and these pockets are responsible for the Cooper instability at $P > P_{c1}$. With tight-binding dispersion (2) at $P > P_{c1}$, there are four ungapped pockets on each of the two sheets of the original Fermi surface: two electron pockets with $E_2(k) = \varepsilon_+(\mathbf{k}) + \sqrt{\varepsilon_-^2(\mathbf{k}) + |\Delta_0|^2} < 0$ at $k_{y\,\max} b = \pi/2,\ 3\pi/2$, and $k_{x\,\max} = k_F$, and two hole pockets with $E_1(k) = \varepsilon_+(\mathbf{k}) - \sqrt{\varepsilon_-^2(\mathbf{k}) + |\Delta_0|^2} > 0$ at $k_{y\,\max} b = 0, \pi$ and $k_{x\,\max} = k_F \pm 2t_b/v_F$ (see Fig. 2). The hole pockets of the new FS are the elongated ellipses, satisfying $E_1(\mathbf{k}) = 0$ and with the main axes along the vectors $\mathbf{k}_x$ and $\mathbf{k}_y$. The two electron pockets are the similar ellipses, rotated in the k_x-k_y plane by the angles

$$\phi_e = \pm \arctan(2t_b b/\hbar v_F). \tag{19}$$

Near the points $\mathbf{k} = \mathbf{k}_{\max}$, where $|\varepsilon_+(\mathbf{k})|$ has a maximum and the small ungapped pockets get formed, dispersion (16) is rewritten as $(\Delta k_y = k_y - k_{y\,\max})$,

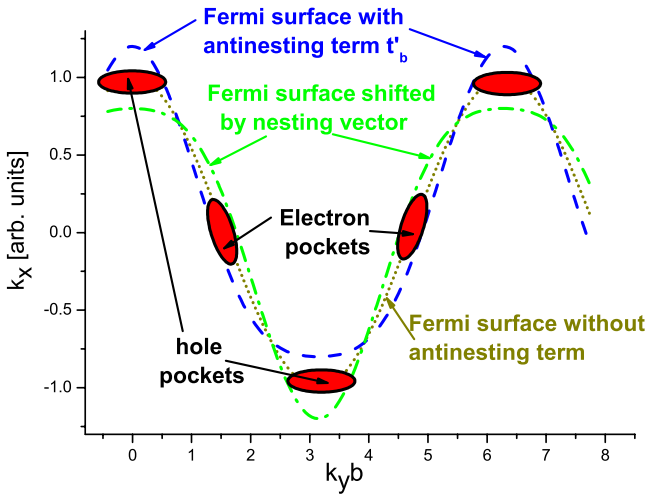

FIG. 2. (Color online) The schematic picture of small open pockets on one Fermi surface sheet, which get formed when the antinesting term ε_+ in Eq. (16) exceeds the DW energy gap Δ_0. The blue dashed line shows the Fermi surface sheet with imperfect nesting, i.e., with $2t_b > \Delta_0$. The green dashed-dotted line shows the other Fermi surface sheet shifted by the nesting vector. If the nesting was perfect, these two lines would coincide. The dotted brown line shows the perfectly nested Fermi surface sheet. The red solid ellipses are the small Fermi surface pockets that appear in the DW state when $2t_b > \Delta_0$, i.e., when the pressure exceeds P_{c1}.

$$E_1(\Delta k_y, \varepsilon_-) \approx -\delta + a_1(\Delta k_y)^2 + b_1\varepsilon_-^2, \tag{20}$$

where using Eq. (2) one obtains

$$\varepsilon_-(\mathbf{k}) \approx v_F(k_x - k_F) - 2t_b b \sin(k_{y\,\max} b)\Delta\mathbf{k}_y/\hbar,$$

$$\delta \equiv |\varepsilon_+(\mathbf{k})|_{\max} - |\Delta_0| = 2t'_b - |\Delta_0|, \tag{21}$$

$$a_1 \approx 4t'_b b^2 \ \text{ and } \ b_1 \approx 1/2\Delta_0. \tag{22}$$

Here δ means the Fermi energy in these small pockets,[36] and the last term in Eq. (21) rotates the electron FS pockets by angle (19).

Without DW ordering, the density of states (DoS) of electrons with quasi-1D dispersion (1) is

$$\rho_0(E_F) = \int \frac{dk_x dk_y}{(2\pi)^2} \delta[\hbar v_F(k_x \pm k_F)] = \frac{1}{\pi\hbar v_F b}.$$

Let us estimate the DoS on the Fermi level in the DW phase when the open pockets just appear (Fig. 3). By definition,[37]

$$\rho(\varepsilon) = -(1/\pi)\mathrm{Im}[\mathrm{Tr}\, G_{\mathrm{ret}}(\varepsilon)]. \tag{23}$$

The retarded Green's function is obtained from Eq. (18) by using the analytical continuation $i\omega \to \varepsilon + i0$. Its substitution into Eq. (23) gives the DoS on the Fermi level (at $\varepsilon = 0$),

$$\rho(E_F) = \sum_{\mathbf{k}} \left(\frac{\varepsilon(\mathbf{k})}{E_1(\mathbf{k})} \delta[E_2(\mathbf{k})] + \frac{\varepsilon(\mathbf{k})}{E_2(\mathbf{k})} \delta[E_1(\mathbf{k})] \right), \tag{24}$$

where $\delta[x]$ is the Dirac δ function. For small FS pockets, i.e., at $\delta \ll \Delta_0$, the residues of Green's function poles

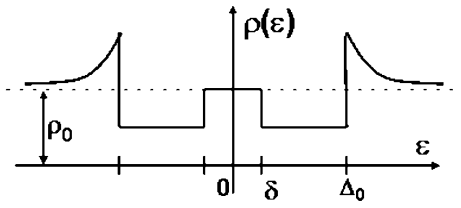

FIG. 3. The schematic picture of the density of states $\rho(\varepsilon)$ near the Fermi level in the DW phase with ungapped FS pockets. On the figure, ρ_0 is the DoS in the metallic phase, Δ_0 is the DW energy gap, and δ is the size of new ungapped pockets [see Eq. (22)].

$$\frac{\varepsilon(\mathbf{k})}{E_1(\mathbf{k})} = \frac{\varepsilon(\mathbf{k})}{E_2(\mathbf{k})} \approx \frac{1}{2},$$

and the contribution of one ungapped FS pocket per one spin orientation is given by

$$\rho_1 = \int \frac{dk_x d\Delta k_y}{(2\pi)^2} \frac{\delta[a_1(\Delta k_y)^2 + b_1\varepsilon_-^2 - \delta]}{2}$$
$$= \int \frac{dxdy/(2\pi)^2}{\hbar v_F\sqrt{a_1 b_1}} \frac{\delta(x^2+y^2-\delta)}{2}$$
$$= \int \frac{dr^2/8\pi}{\hbar v_F b} \delta(r^2-\delta) = \frac{1}{8\pi\hbar v_F b}.$$

There are eight ungapped pockets for dispersion (2), and the total DoS on the Fermi level per one spin component in DW state is the same as without DW ordering,

$$\rho(E_F) = 8\rho_1 = \frac{1}{\pi\hbar v_F b}. \tag{25}$$

This result differs from that in the previously studied models,[5,6] where the electron spectrum on the ungapped parts of the FS does not change after the formation of DW and the DoS on the Fermi level reduces when the DW is formed, so that the SC transition temperature reduces exponentially. In our model, the DoS on the Fermi level in the DW state with open FS pockets is the same as without DW. Therefore, the SC transition temperature in our model does not change so strongly when the DW ordering with ungapped pockets is destroyed completely with the restoration of the metallic state (see Sec. III A for more details). The DoS at the Fermi level also determines many other physical properties. Its schematic view as a function of energy, counted from the Fermi level, is shown in Fig. 3.

C. Stability with respect to superconductivity in the metallic state

In terms of left and right moving electrons, interaction Hamiltonian (5) with coupling functions (6) and (7) has the form

$$\hat{H}_{\text{int}} = \frac{1}{2}\sum_{kk'Q} U_c^b a_\alpha^{\dagger R}(\mathbf{k}+\mathbf{Q}) a_\alpha^L(\mathbf{k}) a_\beta^{\dagger L}(\mathbf{k}'-\mathbf{Q}) a_\beta^R(\mathbf{k}')$$
$$+ \frac{1}{2}\sum_{kk'Q} U_c^f a_\alpha^{\dagger R}(\mathbf{k}+\mathbf{Q}) a_\alpha^R(\mathbf{k}) a_\beta^{\dagger L}(\mathbf{k}'-\mathbf{Q}) a_\beta^L(\mathbf{k}'). \tag{26}$$

With two FS sheets in Eq. (1), it is useful to describe SC in terms of two Gor'kov functions,[37]

$$F^{L(R)R(L)}(X_1,X_2) = \langle T(\hat{\Psi}^{L(R)}(X_1)\hat{\Psi}^{R(L)}(X_2))\rangle, \tag{27}$$

where $X=(\tau,\boldsymbol{r})$ and $\hat{\Psi}^{L(R)}(X)$ are the field operators for the left and right parts of the Brillouin zone formally comprising the electrons with momenta $P_\parallel<0(L)$ and $P_\parallel>0(R)$. The averages in Eq. (27) at $\tau_1=\tau_2+0$,

$$\hat{f}_{\alpha\beta}^{LR}(\mathbf{r}) = \langle\hat{\Psi}_\alpha^L(\mathbf{r})\hat{\Psi}_\beta^R(\mathbf{r})\rangle,$$

$$\hat{f}_{\alpha\beta}^{RL}(\mathbf{r}) = \langle\hat{\Psi}_\alpha^R(\mathbf{r})\hat{\Psi}_\beta^L(\mathbf{r})\rangle, \tag{28}$$

mean the Cooper pair wave function and determine the SC order parameter $\hat{\Delta}_{\text{SC}}(\mathbf{r})$. The symbol "hat" above the functions $\hat{f}^{LR}(\mathbf{r})$ and $\hat{\Delta}_{\text{SC}}(\mathbf{r})$ means that these functions are operators in the spin space. In materials with spatial inversion symmetry, such as $(\text{TMTSF})_2\text{PF}_6$, one has $\hat{f}^{LR}=\pm\hat{f}^{RL}$, and the sign $(\pm)$ depends on whether the SC pairing is singlet (+) or triplet (−). Below we assume the uniform SC order parameter: $\hat{f}_{\alpha\beta}^{LR}(\mathbf{r})=\hat{f}_{\alpha\beta}^{LR}$. In the momentum representation, Eq. (28) is rewritten as

$$\hat{f}_{\alpha\beta}^{LR} = \sum_{\boldsymbol{r}} \langle a_\alpha^L(\mathbf{k}) a_\beta^R(-\mathbf{k})\rangle,$$

$$\hat{f}_{\alpha\beta}^{RL} = \sum_{\boldsymbol{r}} \langle a_\alpha^R(\mathbf{k}) a_\beta^L(-\mathbf{k})\rangle. \tag{29}$$

We introduce the notation for the Cooper bubble,

$$\Pi_d = T\sum_{\mathbf{k},\omega} g^{RR}(\mathbf{k},\mathbf{k},\omega) g^{LL}(-\mathbf{k},-\mathbf{k},-\omega), \tag{30}$$

where Green's functions $g^{RR(LL)}(\boldsymbol{r},\boldsymbol{r},\omega)$ in the metallic state are given by Eq. (18) at $\Delta_0=0$. From Hamiltonian (26) with definition (30) one obtains the Gor'kov equations for the onset of SC,

$$\hat{f}^{LR} = -(U_c^b\hat{f}^{RL} + U_c^f\hat{f}^{LR})\Pi_d,$$

$$\hat{f}^{RL} = -(U_c^b\hat{f}^{LR} + U_c^f\hat{f}^{RL})\Pi_d. \tag{31}$$

Equation (31) is shown schematically in Fig. 4. Summation and subtraction of the two lines in Eq. (31) gives the equations on SC transition temperature T_{c0}^{SC} in the metallic state,

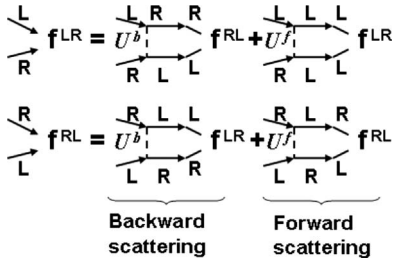

FIG. 4. The diagram equations for the Gor'kov functions $\hat{f}^{LR}$ and $\hat{f}^{RL}$ without DW. The solid lines represent the electron Green's functions: $g^{RR(LL)}(\boldsymbol{k},\omega)$ in the metallic state. The dashed lines represent the short-range e-e interaction U_c^f or U_c^b.

$$\hat{f}^{LR}+\hat{f}^{RL}=-(U_c^f+U_c^b)(\hat{f}^{LR}+\hat{f}^{RL})\Pi_d,$$

$$\hat{f}^{LR}-\hat{f}^{RL}=-(U_c^f-U_c^b)(\hat{f}^{LR}-\hat{f}^{RL})\Pi_d. \tag{32}$$

The first line in Eq. (32) corresponds to the singlet pairing, and the second line to the triplet pairing. Usually, $-U_c^f-U_c^b > U_c^b-U_c^f$, and the singlet SC transition temperature is higher. Equation (32) is rewritten as

$$1=g\Pi_d, \quad g=\max\{-U_c^f-U_c^b, U_c^b-U_c^f\}. \tag{33}$$

Therefore, in our model one has singlet or triplet superconductivity depending on the ratio of the coupling constants U_c^f and U_c^b. The nonmagnetic impurities also suppress the triplet SC ordering. The Cooper bubble Π_d has the well-known logarithmic singularity, appearing after the summation over momenta and frequencies,

$$\Pi_d^{\mathrm{met}}=\Pi_d^{\mathrm{met}}(T)\approx \nu_F \ln(\bar{\omega}/T), \tag{34}$$

where $\bar{\omega}$ is a proper cutoff[37] and $\nu_F=\rho_0(E_F)$ is the density of states at the Fermi level. For quasi-1D electron spectrum (1), $\nu_F=1/\pi\hbar v_F b$. From Eqs. (33) and (34), one obtains the equation for the SC critical temperature T_{c0}^{SC},

$$1\approx g\nu_F \ln(\bar{\omega}/T_{c0}^{\mathrm{SC}}). \tag{35}$$

III. SUPERCONDUCTIVITY IN THE CHARGE-DENSITY WAVE STATE

First, we study the SC instability in the CDW state, where the spin structures of the CDW and SC order parameters do not interfere. As we shall see below in Sec. IV, the results obtained in this section for the spin-singlet superconductivity on the CDW background can be applied with little modification for the triplet superconductivity on the SDW background. The problem of SC instability and the upper critical field H_{c2} on the CDW background is important itself. The organic metal α-$(\mathrm{BEDT\text{-}TTF})_2\mathrm{KHg(SCN)}_4$ is an example in which the interplay between superconductivity and CDW leads to the new SC properties,[9] and there are many other CDW superconductors.[1]

The basic equations for the CDW state without superconductivity are obtained from Eqs. (13)–(22) by removing the spin factor $(\vec{\hat{\sigma}}\vec{l})$ from the nondiagonal elements in Eqs.

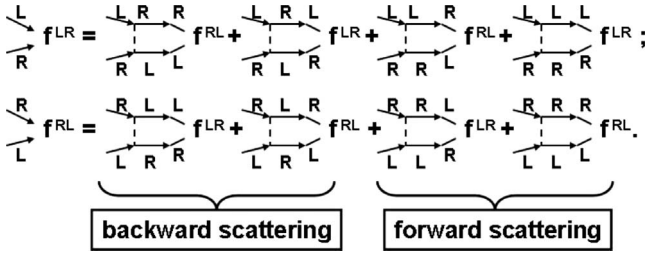

FIG. 5. The diagram equations for the Gor'kov functions $\hat{f}^{LR}$ and $\hat{f}^{RL}$ in the presence of the DW ordering with two coupling constants. The solid lines represent the electron Green's functions $g_n^{R(L)R(L)}(k,\omega)$ in the DW state. The dashed lines represent the short-range e-e interaction, i.e., backward U_c^b or forward U_c^f scattering.

(11)–(13). Thus, the matrix Green's function in the uniform CDW state without SC resembles Eq. (13),

$$\hat{G}\equiv\begin{pmatrix} g^{RR}(\boldsymbol{k},\boldsymbol{k},\omega) & g^{LR}(\boldsymbol{k}-\boldsymbol{Q},\boldsymbol{k},\omega) \\ g^{RL}(\boldsymbol{k},\boldsymbol{k}-\boldsymbol{Q},\omega) & g^{LL}(\boldsymbol{k}-\boldsymbol{Q},\boldsymbol{k}-\boldsymbol{Q},\omega)\end{pmatrix}, \tag{36}$$

with the matrix components given by Eqs. (17) and (18). In addition to term (30), the Cooper bubble on the DW background contains another term, coming from the nondiagonal elements in Green's function (36),

$$\Pi_n=T\sum_{\mathbf{k},\omega} g^{LR}(\mathbf{k}-\mathbf{Q},\mathbf{k},\omega)g^{RL}(-\mathbf{k}+\mathbf{Q},-\mathbf{k},-\omega). \tag{37}$$

Therefore, the Gor'kov equations on the DW background acquire two additional terms as compared to Eq. (31),

$$\hat{f}^{LR}=-(U_c^b\hat{f}^{RL}+U_c^f\hat{f}^{LR})\Pi_d-(U_c^b\hat{f}^{LR}+U_c^f\hat{f}^{RL})\Pi_n,$$

$$\hat{f}^{RL}=-(U_c^b\hat{f}^{LR}+U_c^f\hat{f}^{RL})\Pi_d-(U_c^b\hat{f}^{RL}+U_c^f\hat{f}^{LR})\Pi_n. \tag{38}$$

In writing these equations we use that the spin structure of the Gor'kov functions $\hat{f}^{LR}$ commutes with Green's functions $g^{R(L)R(L)}(\boldsymbol{k},\boldsymbol{k}',\omega)$ on the CDW background. Equation (38) is shown schematically in Fig. 5.

The summation and subtraction of the two lines in Eq. (38) gives the following equations on the SC transition temperature for singlet and triplet pairings, respectively:

$$\hat{f}^{LR}+\hat{f}^{RL}=-(U_c^f+U_c^b)(\hat{f}^{LR}+\hat{f}^{RL})(\Pi_d+\Pi_n),$$

$$\hat{f}^{LR}-\hat{f}^{RL}=-(U_c^f-U_c^b)(\hat{f}^{LR}-\hat{f}^{RL})(\Pi_d-\Pi_n). \tag{39}$$

Below we show that Π_d and Π_n have the same sign and $|\Pi_d+\Pi_n|>|\Pi_d-\Pi_n|$. Therefore, if in the metallic state the transition temperature $T_{c\mathrm{SC}}^{\mathrm{singlet}}$ to singlet SC is higher than $T_{c\mathrm{SC}}^{\mathrm{triplet}}$ to the triplet SC, then on the CDW background $T_{c\mathrm{SC}}^{\mathrm{singlet}}>T_{c\mathrm{SC}}^{\mathrm{triplet}}$ is also valid. For SDW, the interplay between the spin structures of SC and SDW produces important changes (see Sec. IV).

A. Superconductivity instability and transition temperature in the uniform charge-density wave state with ungapped Fermi surface pockets

The equation for the singlet SC transition temperature $T_{c\mathrm{CDW}}^{\mathrm{SC}}$ on CDW background, given by the first line in Eq.

(39), is written down as $K_1 \equiv g(\Pi_d + \Pi_n) = 1$, where for singlet pairing $g = -(U_c^f + U_c^b)$. Using $\varepsilon(\mathbf{k}) = \varepsilon(-\mathbf{k})$ and substituting Eq. (17) into Eq. (18), we obtain

$$K_1 = Tg \sum_{\mathbf{k},\omega_n} \frac{\omega^2 + [\varepsilon_-(\boldsymbol{k}) + \varepsilon_+(\boldsymbol{k})]^2 + |\Delta_0|^2}{[\omega^2 + E_1^2(\boldsymbol{k})][\omega^2 + E_2^2(\boldsymbol{k})]} \tag{40}$$

$$= \frac{Tg}{2} \sum_{\mathbf{k},\omega_n} \left(\frac{1}{\omega^2 + E_1^2(\boldsymbol{k})} + \frac{1}{\omega^2 + E_2^2(\boldsymbol{k})} \right) \tag{41}$$

$$= \frac{g}{v_F} \int_0^{2\pi/b} \frac{b dk_y}{2\pi} \int_{-\bar{\omega}}^{\bar{\omega}} \frac{d\varepsilon_-}{2\pi} \frac{\tanh[E_1(\mathbf{k})/2T]}{E_1(\mathbf{k})}. \tag{42}$$

In writing the second line, Eq. (41), we have substituted Eq. (16) and used the symmetry of the functions $\varepsilon_\pm(k_y)$: $\varepsilon_+(k_y)$ is an even function of k_y and $\int dk_y F(\varepsilon_\pm(k_y)) = 0$ for any odd function $F(\varepsilon)$. Let us now rewrite $K_1 \equiv K_{\mathrm{ult}} + K_{\mathrm{inf}}$, where

$$K_{\mathrm{ult}} \equiv \frac{g}{v_F} \int_0^{2\pi/b} \frac{b dk_y}{2\pi} \int_{|\Delta_0|}^{\bar{\omega}} \frac{d\varepsilon_-}{\pi} \frac{\tanh[E_1(\mathbf{k})/2T]}{E_1(\mathbf{k})}$$

$$\approx [g/\pi v_F] \ln(\bar{\omega}/\Delta_0) \tag{43}$$

contains the ultraviolet logarithmic divergence in expression (42), and

$$K_{\mathrm{inf}} \equiv \frac{g}{v_F} \int_0^{2\pi/b} \frac{b dk_y}{2\pi} \int_0^{|\Delta_0|} \frac{d\varepsilon_-}{\pi} \frac{\tanh[E_1(\mathbf{k})/2T]}{E_1(\mathbf{k})} \tag{44}$$

may contain the infrared logarithmic divergence if there are electron states on the Fermi level. At $P > P_{c1}$ the ungapped electron states appear as small Fermi surface pockets (see Sec. II B and Fig. 2), or as the soliton band.[17] In each case, the formed small "Fermi surface" is subjected to the Cooper instability at rather low temperature, which signifies the possibility for the onset of SC pairing.

Substituting Eq. (20) for $E_1(\boldsymbol{k})$ into Eq. (44) and introducing $r^2 \equiv a_1(\Delta k_y)^2 + b_1 \varepsilon_-^2$, we obtain

$$K_{\mathrm{inf}} \approx \frac{N_P^e g b / v_F}{4\pi \sqrt{a_1 b_1}} \int_0^{\Delta_0} \frac{\tanh[(\delta - r^2)/2T]}{\delta - r^2} dr^2$$

$$\approx \frac{N_P^e g}{2\pi v_F \sqrt{2t_b'/\Delta_0}} \ln[C\sqrt{\Delta_0 \delta}/T], \tag{45}$$

where $C \sim 1$ is a numerical constant and N_P^e is the number of ungapped electron pockets on one FS sheet. With tight-binding dispersion (2), at $2t_b' > \Delta_0$ in each Brillouin zone $N_P^e = 2$ (see Fig. 2). Thus, when the small pockets just appear, i.e., when $0 < 2t_b'/\Delta_0 - 1 \ll 1$,

$$K_1 \approx \frac{g}{\pi v_F} [\ln(\bar{\omega}/\Delta_0) + \ln(C\sqrt{\Delta_0 \delta}/T)]. \tag{46}$$

Comparing Eqs. (46) and (35) one obtains that the SC critical temperature $T_{c\mathrm{CDW}}^{\mathrm{SC}}$ in the CDW state is related to the SC transition temperature T_{c0}^{SC} without CDW as

$$T_{c\mathrm{CDW}}^{\mathrm{SC}} \approx C T_{c0}^{\mathrm{SC}} \sqrt{\delta/\Delta_0}. \tag{47}$$

This result differs from Eqs. 3.5 and 3.7 of Ref. 6, where $T_{c\mathrm{CDW}}^{\mathrm{SC}}$ is exponentially smaller than T_{c0}^{SC}. The origin of this difference was explained at the end of Sec. II B, where the DoS on the Fermi level in the DW state with small open pockets and in the metallic state were shown to be approximately the same. The assumption that the electron spectrum in the ungapped FS pockets does not change after the formation of DW, used in Refs. 5 and 6, is not valid, especially when the ungapped FS pockets are small. For quasi-1D tight-binding dispersion, given by Eqs. (1) and (2), the SC transition temperature on the CDW background with ungapped FS pockets $T_{c\mathrm{CDW}}^{\mathrm{SC}}$ is only slightly less than T_{c0}^{SC}.

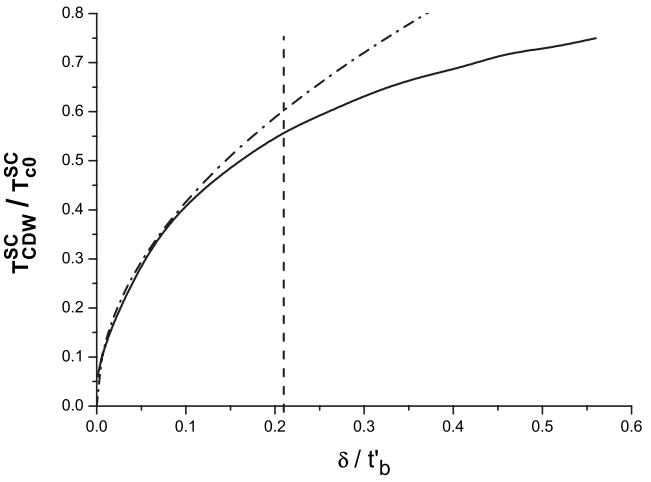

FIG. 6. The SC transition temperature $T_{c\mathrm{DW}}^{\mathrm{SC}}$ on the DW background in the pocket scenario. The solid line shows the ratio $T_{c\mathrm{DW}}^{\mathrm{SC}}/T_{c0}^{\mathrm{SC}}$, calculated numerically from Eq. (42), as function of the size δ of the ungapped Fermi surface pockets. The dashed-dotted line represents analytical formula (47) with the numerically calculated constant $C \approx 1.86$. The approximate experimental value $\delta_{\max}$ for $(\mathrm{TMTSF})_2\mathrm{PF}_6$ is denoted by the vertical dashed line.

Equations (43)–(47) were derived following Ref. 17 with logarithmic accuracy, i.e., assuming $\ln(\delta/T) \gg 1$ and $\ln(\Delta_0/\delta) \gg 1$. This accuracy is not sufficient to determine the constant C. For a more accurate estimate of the transition temperature $T_{c\mathrm{CDW}}^{\mathrm{SC}}$, we calculated integral (42) numerically for the particular dispersion (2). This calculation confirms approximate formula (47) at $\delta \ll \Delta_0$ and gives the value of the constant $C \approx 1.86$ (see Fig. 6). At $\delta/t_b' \ll 1$ the analytical and numerical results coincide, while at $\delta \sim t_b'$ the ratio $T_{c\mathrm{CDW}}^{\mathrm{SC}}(\delta)/T_{c0}^{\mathrm{SC}}$ tends to saturate, being always less than unity. In agreement with Eq. (47), the ratio $T_{c\mathrm{CDW}}^{\mathrm{SC}}/T_{c0}^{\mathrm{SC}}$ is almost independent of T_{c0}^{SC}. Equation (47) and the numerical result in Fig. 6 applies only at $0 < \delta < \delta_{\max}$. At $\delta \geq \delta_{\max}$ the DW state is completely destroyed, and the system is in the metallic or SC state. The value $\delta_{\max}$ depends on the electron dispersion,[16] on the form of e-e interaction, and on many other factors. In particular, the critical fluctuations at $P \approx P_{c1}$ and $P \approx P_c$ may considerably influence the phase diagram. The back action of superconductivity on DW, disregarded in the present analysis, also affects the value of $\delta_{\max}$. Therefore, we do not calculate the value of $\delta_{\max}$ but take it from experiment. In $(\mathrm{TMTSF})_2\mathrm{PF}_6$ from the phase diagram in Fig. 7 of Ref. 8, one estimates $\delta_{\max}/t_b' \sim 0.2$. In α-$(\mathrm{BEDT\text{-}TTF})_2\mathrm{KHg(SCN)}_4$ the interval $0 < \delta < \delta_{\max}$ is much larger, and $P_{c1} \approx P_c/2$ (see Fig. 9 of Ref. 9). In Fig. 6

the dashed line shows the approximate experimental value of $\delta_{\max}$ for $(TMTSF)_2PF_6$.

The above analytical and numerical estimations show that the CDW state with ungapped pockets on the Fermi surface is always unstable toward the formation of the superconductivity, and the SC transition temperature $T_{c\mathrm{CDW}}^{\mathrm{SC}}$ on the CDW background is not very low, being slightly less than the SC transition temperature T_{c0}^{SC} without CDW. The formation of the ungapped pockets in the CDW state due to the increase in the antinesting term at $P>P_{c1}$ is, usually, accompanied by the reduction in the CDW energy gap Δ_0 and, hence, by the fast growth of the size $\delta(P)$ of the ungapped FS pockets. Then, from Eq. (47) we obtain that the SC critical temperature $T_{c\mathrm{CDW}}^{\mathrm{SC}}$ also grows very rapidly at $P>P_{c1}$. In experiment, this fast growth of $T_{c\mathrm{CDW}}^{\mathrm{SC}}(P)$ above P_{c1} may be similar to the jump of $T_{c\mathrm{CDW}}^{\mathrm{SC}}$ from zero to some finite value.

The critical fluctuations and change in the effective e-e interaction,[24–26] accompanying the transition from the DW to metallic state in the whole pressure interval $P_{c1}\lesssim P\lesssim P_{c1}$, may considerably increase the SC transition temperature $T_{c\mathrm{CDW}}^{\mathrm{SC}}$ and influence the dependence $T_{c\mathrm{CDW}}^{\mathrm{SC}}(P)$. DW also affects the screening of the Coulomb interaction, which changes the effective e-e coupling and the SC transition temperature. Even a small change in the e-e coupling constant leads to dramatic changes in the SC transition temperature.[37] An accurate calculation of $T_{c\mathrm{CDW}}^{\mathrm{SC}}(P)$ on the DW background must take these effects into account, being beyond the scope of the present paper. However, the obtained result that the formation of the DW energy gap with only small ungapped FS pockets does not reduce the SC transition temperature exponentially, but only by a factor of $\sim\sqrt{\delta/\Delta_0}$, is very important for the possibility of SC on the DW background.

B. Upper critical field H_{c2} in the superconductivity state on the uniform charge-density wave background

The upper critical field in superconductors with intrinsic DW ordering was considered theoretically in the model,[38] where the DW gap appears only on those FS sections, where the nesting condition is fulfilled, while on the rest of FS the electron spectrum has no singularities. This is not the case for our model (see Sec. II), where the dispersion of the ungapped electrons in DW state have a singularity at $P\to P_{c1}$, which affect the SC properties and H_{c2}. Other calculations[39,40] of H_{c2} in DW superconductors also use models very different from the one considered in Sec. II.

To calculate the upper critical field H_{c2}, let us use the Ginzburg-Landau (G-L) approximation. The main contribution to the gradient term comes from the ungapped pockets of the Fermi surface ($|\varepsilon_+(\boldsymbol{k})|>\Delta_0$). For arbitrary electron dispersion, the G-L functional was derived in Ref. 41. The order parameter in the general form is a function of two wave vectors,

$$\Delta(\mathbf{k}_1,\mathbf{k}_2)=\Delta_{\mathbf{q}}(\mathbf{k})=\Delta(\mathbf{q})\psi(\mathbf{k}),$$

where the vector $\mathbf{q}=k_1+k_2$ gives the spatial modulation of the SC order parameter $\Delta(\mathbf{r})=\int d\mathbf{q}\Delta(\mathbf{q})e^{i\mathbf{q}r}$ and $\mathbf{k}=\mathbf{k}_1$ is the momentum of an electron in a Cooper pair. In the case of s pairing, $\psi(\mathbf{k})=\mathrm{const}=1$. For triplet pairing $\Delta_{\mathbf{q}}(\mathbf{k})=-\Delta_{\mathbf{q}}(-\mathbf{k})$ and for quasi-1D dispersion (2) with two separated FS sheets, we may take $\psi(\mathbf{k})=\mathrm{sgn}(k_x)$. To calculate the gradient term in the Ginzburg-Landau expansion, we use Eq. (11) of Ref. 41, which gives the G-L equation for the order parameter in the form

$$\sum_{j,k}\frac{1}{2m_{jk}}[\nabla_j+2ieA_j(\mathbf{r})][\nabla_k+2ieA_k(\mathbf{r})]\Delta(\mathbf{r})+T\left[\frac{T_c^{\mathrm{SC}}-T}{T_c^{\mathrm{SC}}}-f|\Delta(\mathbf{r})|^2\Delta(\mathbf{r})\right]=0, \tag{48}$$

where $A_j(\mathbf{r})$ is the vector potential,

$$\frac{1}{m_{jk}}=\frac{7\xi(3)}{12\pi^2T}\int \mathbf{v}_j\mathbf{v}_k\psi^2(\mathbf{k})\frac{d\sigma_F}{|\mathbf{v}|}\Bigg/\int\frac{d\sigma_F}{|\mathbf{v}|}\equiv\frac{7\xi(3)}{12\pi^2T}\frac{\int \mathbf{v}_j\mathbf{v}_k\psi^2(\mathbf{k})d^3\mathbf{k}\,\delta[E(\mathbf{k})-E_F]}{\int\psi^2(\mathbf{k})d^3\mathbf{k}\,\delta[E(\mathbf{k})-E_F]}, \tag{49}$$

$$f=\frac{7\xi(3)}{8(\pi T)^2}\int\psi^4(\mathbf{k})\frac{d\sigma_F}{|v_F^*|}, \tag{50}$$

and $\int d\sigma_F$ is the integral over the Fermi surface in the momentum space. Since the G-L equation (48) was derived at $T_c^{\mathrm{SC}}-T\ll T_c^{\mathrm{SC}}$, one can replace T by T_c^{SC} in Eqs. (49) and (50). Introducing the notations

$$k_x^*=k_x-k_F;k_y^*\equiv\Delta k_y(2b\sqrt{2t_b\Delta_0}/\hbar v_F),$$

one rewrites dispersion (20) for the hole pockets of the FS as

$$E(\mathbf{k}^*)=\frac{(\hbar v_F)^2}{2\Delta_0}[k_y^{*2}+k_x^{*2}]-\delta. \tag{51}$$

The Fermi surface, $E(\mathbf{k}^*)=0$, is parameterized by the angle ϕ, where $\tan\phi\equiv k_y^*/k_x^*$. The quasiparticle velocity on the FS is a function of this angle,

$$v_x=v_F\sqrt{2\delta/\Delta_0}\cos\phi;$$

$$v_y=(4b/\hbar)\sqrt{\delta t_b}\sin\phi.$$

Performing the integrations in Eq. (49), we obtain the contribution from each hole pocket to tensor (49),

$$\left(\frac{1}{m_{xx}}\right)_h=\frac{7\xi(3)v_F^2}{12\pi^2T_c^{\mathrm{SC}}}\left(\frac{\delta}{\Delta_0}\right),$$

$$\left(\frac{1}{m_{yy}}\right)_h=\frac{14\xi(3)b^2t_b'\delta}{3\pi^2\hbar^2T_c^{\mathrm{SC}}},\quad\left(\frac{1}{m_{xy}}\right)_h=0. \tag{52}$$

This mass tensor is very anisotropic:

$$\left(\frac{m_{yy}}{m_{xx}}\right)_h=\frac{\hbar^2v_F^2}{8t_b\Delta_0b^2}\sim\left(\frac{\hbar v_F}{2bt_b}\right)^2\gg 1.$$

The contribution from the electron pockets can be obtained via the rotation of tensor (52) by angles (19),

$$\left(\frac{1}{m_{xx}}\right)_e = \left(\frac{1}{m_{xx}}\right)_h \cos^2\phi_e + \left(\frac{1}{m_{yy}}\right)_h \sin^2\phi_e,$$

$$\left(\frac{1}{m_{yy}}\right)_e = \left(\frac{1}{m_{xx}}\right)_h \sin^2\phi_e + \left(\frac{1}{m_{yy}}\right)_h \cos^2\phi_e.$$

The nondiagonal elements $(1/m_{xy})_e$ vanish after the summation over two electron pockets, which are rotated in the opposite directions. The total G-L mass tensor is

$$\frac{1}{m_{ij}} = 4\left[\left(\frac{1}{m_{ij}}\right)_e + \left(\frac{1}{m_{ij}}\right)_h\right],$$

and using $|\phi_e| = \arctan(2t_b b/\hbar v_F) \ll 1$, we obtain

$$\frac{1}{m_{xx}} \approx \frac{14\xi(3)v_F^2}{3\pi^2 T_c^{SC}}\left(\frac{\delta}{\Delta_0}\right),$$

$$\frac{1}{m_{yy}} \approx \frac{7\xi(3)v_F^2}{3\pi^2 T_c^{SC}}\left(\frac{\delta}{\Delta_0}\right)\left(\frac{2t_b b}{\hbar v_F}\right)^2. \tag{53}$$

From the Ginzburg-Landau equation, one obtains the i component of the upper critical field,

$$H_{c2}^i = e_{ijk}\frac{(T_c^{SC}-T)c}{e\hbar}\sqrt{m_j m_k}, \tag{54}$$

where e_{ijk} is the antisymmetric tensor of rang 3. For $H\|z$, the substitution of Eq. (53) into Eq. (54) gives

$$H_{c2}^z = C_1\left(\frac{T_c^{SC}}{\delta}\right)\frac{c(T_c^{SC}-T)}{bv_F e}, \tag{55}$$

where

$$C_1 = \frac{3\pi^2}{7\xi(3)\sqrt{2}}\left(\frac{\Delta_0}{2t_b}\right). \tag{56}$$

The estimate of constant (56) is very sensitive to electron dispersion (2), e.g., to the presence of the fourth harmonic $2t_4\cos(4k_y b)$ in Eq. (2). The fourth harmonic with $t_4/t_2 > 0$ increases the size δ of the ungapped hole pockets at $k_y b \approx \pi n$ by $2t_4$, reducing by the same amount the size of the electron pockets at $k_y b \approx \pi(n+1/2)$. If $2t_4 > \delta$, the electron pockets disappear, and only the hole pockets contribute to mass tensor (49). The total mass tensor is then very anisotropic and given by Eq. (52) multiplied by the number of the hole pockets. Its substitution into Eq. (54) gives (we take $\Delta_0/2t_b \approx 1$)

$$C_1 = 3\pi^2/14\xi(3) = 1.76, \tag{57}$$

which is greater than Eq. (56) by a factor of $\sim t_b/t_b'$. The similar increase in the constant C_1 also appears if the DW wave vector $\mathbf{Q}$ shifts from $\mathbf{Q}_0 = (2k_F, \pi/b)$, so that the electron pockets disappear, while the size δ of the hole pockets increases. Accurate calculation of the constant C_1 requires the detailed knowledge of electron dispersion.

According to Eq. (55), H_{c2}^z diverges as $P - P_{c1} \to 0$, because $\delta \propto P - P_{c1}$.[36] Assuming $T_c^{SC} \approx$ const, as it is observed in the organic superconductors $(TMTSF)_2PF_6$ and α-$(BEDT\text{-}TTF)_2KHg(SCN)_4$, one obtains

$$H_{c2}^z \propto 1/(P - P_{c1}). \tag{58}$$

In our simplified model (47), $T_c^{SC} \propto \sqrt{\delta} \propto \sqrt{P - P_{c1}}$, and from Eq. (55) one obtains the square-root divergence of the slope $dH_{c2}^z(T)/dT$ in the vicinity of transition temperature $T = T_c^{SC}$: $dH_{c2}^z(T)/dT \approx H_{c0}/\sqrt{P/P_{c1} - 1}$. However, the calculation of the SC transition temperature is always based on many approximations, being a notoriously difficult problem. Thus, in the derivation of Eq. (47), we disregarded the renormalization of the e-e coupling by the DW critical fluctuations. Therefore, the dependence $T_c^{SC}(P)$ should be rather taken from experiment. The physical reason for enhancement (58) of the upper critical field H_{c2} in the vicinity of P_{c1} is the increase in the effective mass in the Ginzburg-Landau equations [see Eqs. (52) and (53)], which comes from the strong change in the quasiparticle dispersion (namely, from the reduction of their mean-square velocity) on the Fermi level in the ungapped FS pockets.

The divergence of H_{c2}^z as the pressure approaches P_{c1} has been observed in the mixed state in $(TMTSF)_2PF_6$ (see Fig. 2 of Ref. 14) and also in α-$(BEDT\text{-}TTF)_2KHg(SCN)_4$ (see Figs. 5 and 6 of Ref. 9). To explain this dependence $H_{c2}^z(P - P_{c1})$ in the scenario of the macroscopic spatial phase separation,[14] the width d_S of the superconducting domains must be taken much smaller than the SC coherence length ξ_{SC}, because in a thin type-II-superconductor slab of thickness $d_s \ll \xi_{SC}$, the upper critical field H_{c2} is higher than in the bulk superconductor by a factor (see Eq. 12.4 of Ref. 42) of

$$H_{c2}/H_{c2}^0 \approx \sqrt{12}\xi_{SC}/d_s. \tag{59}$$

In the discussion in Ref. 14, the penetration length λ instead of the coherence length ξ_{SC} enters the expression for H_{c2} in a thin superconducting slab, which is only correct for type-I superconductors. If $d_s \ll \xi_{SC}$, the domain size d_s is of the same order as the DW coherence length, which may cost additional energy because of the change in the DW structure. Then, the soliton scenario[17] of the DW/SC structure is possible.

We now make some quantitative comparison with experiment to check if the proposed model is reasonable. In $(TMTSF)_2PF_6$ the Fermi velocity $v_F \approx 2\times 10^7$ cm/s, the interchain spacing $b \approx 7.7$ Å, and $\Delta_0/2t_b \approx t_b/t_b \approx 0.1$. Substituting this and $\delta \approx T_c^{SC}$ into Eq. (55) gives the slope $dH_{c2}^z/dT \approx 1$ T/K, in a reasonable agreement with the experimental data at $P \to P_{c1}$ (see Fig. 2 of Ref. 14).

In α-$(BEDT\text{-}TTF)_2KHg(SCN)_4$, the Fermi velocity[43] $v_F \approx 6.5\times 10^6$, the lattice constant[44] $b \approx 10$ Å, the SC and CDW transition temperatures[9] $T_c^{SC} \approx 0.1$ K, and $T_c^{CDW} \approx 8$ K. Although the original Fermi surface in this compound possesses the quasi-two-dimensional (2D) pockets in addition to the quasi-1D sheets subjected to the CDW instability, the quasi-1D FS sheets seem to play an important role in the formation of SC, because superconductivity appears in the presence of CDW (at $P < P_c$) with approximately the same transition temperature T_c^{SC} as in the absence of CDW at $P > P_c$. Hence, SC and CDW share the same quasi-1D conducting band. In this compound, $P_c \approx 2.5$ kbar,[9] while P_{c1} and $\delta(P)$ are not known; probably, even at ambient pressure, $P > P_{c1}$ and $\delta \lesssim \Delta_0$. Substitution of $\delta \approx \Delta_0/2$ into Eq. (55)

gives the estimate $dH_{c2}^{z}/dT \approx (1-T/T_c^{SC}) \times 3.2$ mT, in agreement with experiment (see Fig. 5 of Ref. 9).

The upper critical field H_{c2} along the conducting x-y planes in the layered quasi-1D superconductors was estimated in Ref. 45. The similar calculation can be applied to our case provided the dispersion along the y and z directions is known accurately.

IV. SUPERCONDUCTING INSTABILITY IN THE SPIN-DENSITY WAVE STATE

Green's functions in the SDW state are given by Eqs. (13)–(18), and the Gor'kov equations for SC in the SDW state, shown schematically in Fig. 5, are written down as

$$\hat{f}^{LR} = -TU_c^b \sum_{\mathbf{k},\omega} [g^{RR}(\mathbf{k},\mathbf{k},\omega)\hat{f}^{RL}g^{LL}(-\mathbf{k},-\mathbf{k},-\omega)^T + g^{LR}(\mathbf{k} - \mathbf{Q},\mathbf{k},\omega)(\vec{\hat{\sigma}}\vec{l})\hat{f}^{LR}(\vec{\hat{\sigma}}\vec{l})^T g^{RL}(\mathbf{Q}-\mathbf{k},-\mathbf{k},-\omega)] - TU_c^f \sum_{\mathbf{k},\omega} [g^{LL}(-\mathbf{k},-\mathbf{k},-\omega)\hat{f}^{LR}g^{RR}(\mathbf{k},\mathbf{k},\omega)^T + g^{RL}(-\mathbf{k}+\mathbf{Q},-\mathbf{k},-\omega)(\vec{\hat{\sigma}}\vec{l})\hat{f}^{RL}(\vec{\hat{\sigma}}\vec{l})^T g^{LR}(\mathbf{k}-\mathbf{Q},\mathbf{k},\omega)] \tag{60}$$

and

$$\hat{f}^{RL} = -TU_c^b \sum_{\mathbf{k},\omega} [g^{LL}(-\mathbf{k},-\mathbf{k},-\omega)\hat{f}^{LR}g^{RR}(\mathbf{k},\mathbf{k},\omega)^T + g^{RL}(\mathbf{Q}-\mathbf{k},-\mathbf{k},-\omega)(\vec{\hat{\sigma}}\vec{l})\hat{f}^{RL}(\vec{\hat{\sigma}}\vec{l})^T g^{LR}(\mathbf{k}-\mathbf{Q},\mathbf{k},\omega)] - TU_c^f \sum_{\mathbf{k},\omega} [g^{RR}(\mathbf{k},\mathbf{k},\omega)\hat{f}^{RL}g^{LL}(-\mathbf{k},-\mathbf{k},-\omega)^T + g^{LR}(\mathbf{k}-\mathbf{Q},\mathbf{k},\omega)(\vec{\hat{\sigma}}\vec{l})\hat{f}^{LR}(\vec{\hat{\sigma}}\vec{l})^T g^{RL}(\mathbf{Q}-\mathbf{k},-\mathbf{k},-\omega)]. \tag{61}$$

The spin structure of the Gor'kov functions $\hat{f}^{LR}$, which depend on the type of SC pairing, interferes with the spin structure $(\vec{\hat{\sigma}}\vec{l})$ of the SDW order parameter. This fact considerably changes the properties of SC on the SDW background as compared to those on the CDW background, studied in Sec. III.

With notations (30) and (37), Eqs. (60) and (61) are rewritten as

$$\hat{f}^{LR} + \hat{f}^{RL} = -T(U_c^b + U_c^f)[\Pi_d(\hat{f}^{RL} + \hat{f}^{LR}) + \Pi_n(\vec{\hat{\sigma}}\vec{l})(\hat{f}^{LR} + \hat{f}^{RL}) \times (\vec{\hat{\sigma}}\vec{l})^T], \tag{62}$$

$$\hat{f}^{LR} - \hat{f}^{RL} = -T(U_c^b - U_c^f)[\Pi_d(\hat{f}^{RL} - \hat{f}^{LR}) + \Pi_n(\vec{\hat{\sigma}}\vec{l})(\hat{f}^{LR} - \hat{f}^{RL}) \times (\vec{\hat{\sigma}}\vec{l})^T]. \tag{63}$$

A. Superconductivity transition temperature

1. Singlet pairing

For spin-singlet paring, $\hat{f}^{LR} = \hat{f}^{LR} = \hat{\sigma}_y f^{LR}$. Since

$$\hat{\sigma}_y(\vec{\hat{\sigma}}\vec{l})^T = -(\vec{\hat{\sigma}}\vec{l})\hat{\sigma}_y, \tag{64}$$

Eq. (62) becomes

$$f^{LR} + f^{RL} = -(U_c^b + U_c^f)(f^{LR} + f^{RL})(\Pi_d - \Pi_n). \tag{65}$$

Substituting Eqs. (30) and (37) into Eq. (62) and using $\varepsilon(\mathbf{k}) = \varepsilon(-\mathbf{k})$, we rewrite Eq. (65) as $K_{\mathrm{SDW}}^s = 1$, where

$$K_{\mathrm{SDW}}^s = Tg \sum_{\mathbf{k},\omega_n} \frac{\omega^2 + [\varepsilon_-(\mathbf{k}) + \varepsilon_+(\mathbf{k})]^2 - |\Delta_0|^2}{[\omega^2 + E_1^2(\mathbf{k})][\omega^2 + E_2^2(\mathbf{k})]} = 1. \tag{66}$$

This formula differs from the corresponding Eq. (40) for CDW in the sign before $|\Delta_0|^2$ in the numerator. This sign change, coming from the interplay between the spin structures of SDW and SC order parameters [Eq. (64)], is crucial for the SC transition temperature. As in the case of CDW, the ungapped pockets of the FS appear when $|\varepsilon_+(\mathbf{k})|_{\max} > |\Delta_0|$, and these pockets are responsible for the low-energy logarithmic singularity of K_1 at $T \to 0$. If the system is close to the phase transition at $P = P_{c1}$, where these pockets just appear, the antinesting term in the electron dispersion only slightly exceeds the SDW gap, and $|\varepsilon_+(\mathbf{k})|_{\max} - |\Delta_0| = \delta \ll |\Delta_0|$. Then in these ungapped pockets $|\varepsilon_-(\mathbf{k})| \sim \delta \ll |\Delta_0|$, and the numerator in Eq. (66) near $\omega \to 0$ has the smallness $\delta/|\Delta_0| \ll 1$ as compared to the case of CDW. This leads to the same smallness of the logarithmically singular term in K_{SDW}^s at $T \to 0$. Instead of Eq. (42), one now obtains

$$K_{\mathrm{SDW}}^s \approx \frac{g}{2} \sum_{\mathbf{k}} \frac{\tanh[E_1(\mathbf{k})/2T]}{E_1(\mathbf{k})} \left(1 - \frac{4|\Delta_0|^2}{E_2^2(\mathbf{k})}\right). \tag{67}$$

When the ungapped pockets are small, the extra factor $[1 - 4|\Delta_0|^2/E_2^2(\mathbf{k})] \sim \delta/\Delta_0 \ll 1$ makes the infrared-divergent term in expression (67) much smaller than that in Eq. (42) for the CDW background. Therefore, the spin-singlet SC transition temperature on the SDW background is exponentially smaller as compared to Eq. (47):

$$T_{c\mathrm{SDW}}^{\mathrm{SC}} \sim \sqrt{\Delta_0 \delta}(T_{c0}^{\mathrm{SC}}/\Delta_0)^{(\Delta_0/\delta)}. \tag{68}$$

Estimates (47) and (68) depend strongly on the electron dispersion.

2. Triplet pairing

The smallness $\sim \delta/\Delta_0$ of the numerator in Eq. (66), emerging for the spin-singlet SC pairing on the SDW background, does not necessarily appear for spin-triplet paring. The triplet order parameter has the spin structure $\hat{f}^{LR} = \hat{\sigma}_y(\hat{\sigma}\tilde{\mathbf{d}})f^{LR}$. Substituting it together with $f^{RL} = -f^{LR}$ into Eq. (63), using $(\vec{\hat{\sigma}}\vec{l})(\hat{\sigma}\tilde{\mathbf{d}}) = -(\hat{\sigma}\tilde{\mathbf{d}})(\vec{\hat{\sigma}}\vec{l}) + 2(\tilde{\mathbf{d}}\vec{l})$ and

$$(\vec{\hat{\sigma}}\vec{l})(\hat{\sigma}\tilde{\mathbf{d}})\hat{\sigma}_y(\vec{\hat{\sigma}}\vec{l})^T = (\hat{\sigma}\tilde{\mathbf{d}})\hat{\sigma}_y - 2(\tilde{\mathbf{d}}\vec{l})(\vec{\hat{\sigma}}\vec{l})\hat{\sigma}_y, \tag{69}$$

we obtain the self-consistency equation

$$(f^{LR} - f^{RL})(\hat{\sigma}\tilde{\mathbf{d}}) = (U_c^b - U_c^f)(f^{LR} - f^{RL}) \times \{(\hat{\sigma}\tilde{\mathbf{d}})\Pi_d - [(\hat{\sigma}\tilde{\mathbf{d}}) - 2(\tilde{\mathbf{d}}\vec{l})(\vec{\hat{\sigma}}\vec{l})]\Pi_n\}. \tag{70}$$

For $\tilde{\mathbf{d}} \| \vec{l}$ the equation on SC transition temperature is the

same as in the case of singlet SC on the CDW background [see the first line of Eq. (39)] with only the change of the coupling constant from $U_c^b+U_c^f$ to $U_c^b-U_c^f$. Hence, at $U_c^f \ll U_c^b$, the SC transition temperature T_c^{SC} for $\tilde{\mathbf{d}}\|\vec{l}$ is approximately given by Eq. (47). For $\tilde{\mathbf{d}}\perp\vec{l}$ one obtains the smallness $\sim\delta/\Delta_0$ of the infrared-divergent term in the Cooper bubble, similar to the case of spin-singlet SC on the SDW background. Then the SC transition temperature T_c^{SC} is roughly given by Eq. (68), being exponentially smaller than in the case $\tilde{\mathbf{d}}\|\vec{l}$. For other mutual orientation of vectors $\tilde{\mathbf{d}}$ and $\vec{l}$, the spin structures of the left and right parts of Eq. (70) do not coincide, which means the possible mixing of singlet and triplet SC states, similar to that in the model of Ref. 46.

B. Upper critical field

As we have shown above, the spin-singlet superconductivity, appearing on the SDW background, has vanishing critical temperature. Hence, we consider only the triplet superconductivity at $\tilde{\mathbf{d}}\|\vec{l}$, which corresponds to the highest critical temperature. For the triplet superconductivity, the paramagnetic spin effect of magnetic field does not necessarily lead to the suppression of superconductivity, and the upper critical field H_{c2} is completely determined by the orbital electron motion. In the scenario of ungapped pockets, the upper critical field H_{c2} on SDW background at $\tilde{\mathbf{d}}\|\vec{l}$ is approximately the same as for SC on the CDW background and is given by Eq. (55).

V. SUMMARY

We investigated the structure and the properties of superconductivity, appearing on the uniform DW background and sharing with DW the common conducting band. The DW instability has two main effects on the SC state. First, it renormalizes the e-e coupling, which affects the SC transition temperature and the type of pairing. Second, the DW background changes the quasiparticle dispersion, which also influences the critical temperature, type of pairing, upper critical field, etc. The former influence has been extensively investigated in a number of papers (see the review papers[25,26] and references therein). It was found that the renormalization of the e-e interaction by the critical DW fluctuations assists the unconventional SC pairing. However, the renormalized e-e interaction depends strongly on the bare e-e coupling functions, which are not usually known with sufficient accuracy. In this paper we focus on the second part of the problem, i.e., on the influence of the DW on the quasiparticle dispersion and, hence, on the SC properties.

The onset of superconductivity requires ungapped electron states on the Fermi level, which appear at pressure $P>P_{c1}$, i.e., when the nesting of the FS is spoiled. There are two possible microscopic structures of the background DW state with such ungapped states on the Fermi level: (a) the DW energy gap does not cover the whole Fermi surface, i.e., there are ungapped FS pockets; and (b) the DW order parameter is not spatially uniform, and the soliton band gets formed.[17] In this paper the first scenario is considered in detail. The approach in Ref. 17 is generalized to the more realistic e-e interaction, which includes two coupling constants. It is shown, that the electron dispersion in the ungapped FS pockets on the DW background is strongly different from that in the metallic state, so that even very small ungapped FS pockets create rather high DoS on the Fermi level. This fact makes our results very dissimilar to many previous theoretical approaches, where the electron dispersion on the ungapped parts of FS in DW state was taken the same as in the metallic state.[5–7,38,39,47] For tight-binding dispersion, given by Eqs. (1) and (2), the DoS on the Fermi level in the DW state with small ungapped FS pockets is the same as in the metallic state without DW [see Eq. (25)]. Therefore, the SC transition temperature $T_{c\mathrm{DW}}^{SC}$ on the DW background with such ungapped FS pockets (i.e., at pressure $P>P_{c1}$) is not exponentially smaller than the SC transition temperature T_{c0}^{SC} in the metallic state [see Eq. (47)], and the quantum critical fluctuations at $P\approx P_{c1}$ may increase $T_{c\mathrm{DW}}^{SC}$ to a value even higher than T_{c0}^{SC}.

The DW background considerably changes the SC properties. The upper critical field H_{c2} has unusual pressure dependence [see Eq. (58)] and may considerably exceed H_{c2} without DW background. According to Eqs. (55) and (58), H_{c2} even diverges as $P\to P_{c1}$; this divergence is cut off at $\delta\sim T_c^{SC}$. The SDW background strongly suppresses the spin-singlet superconductivity, while the triplet SC with certain spin polarization ($\tilde{\mathbf{d}}\|\vec{l}$) on the SDW background behaves similarly as the singlet SC on the CDW background. This means that the SDW background spares the formation of triplet superconductivity compared to the spin-singlet SC. If both types of SC are possible, the system with SDW background will choose the triplet SC, even if it would choose singlet SC without SDW background. The results obtained are in good agreement with experimental observations in the two organic metals $(TMTSF)_2PF_6$ and α-$(BEDT\text{-}TTF)_2KHg(SCN)_4$, where SC coexists with SDW and CDW states respectively, giving an alternative to the explanation in Ref. 14 of the unusual pressure dependence of H_{c2} in $(TMTSF)_2PF_6$ and some other compounds.

ACKNOWLEDGMENTS

The work was supported by RFBR Grants No. 06-02-16551 and No. 06-02-16223 and by Grant No. MK-4105.2007.2. The author thanks the Visitor Program of the Max-Planck-Institut für Physik Komplexer Systeme, Dresden, Germany.

*Also at Institut Laue-Langevin, Grenoble, France. grigorev@itp.ac.ru

[1] A. M. Gabovich, A. I. Voitenko, J. F. Annett, and M. Ausloos, Supercond. Sci. Technol. **14**, R1 (2001).

[2] K. Levin, D. L. Mills, and S. L. Cunningham, Phys. Rev. B **10**, 3821 (1974).

[3] C. A. Balseiro and L. M. Falicov, Phys. Rev. B **20**, 4457 (1979).

[4] L. Miláns del Bosch and Félix Yndurain, Phys. Rev. B **41**, 2540 (1990).

[5] Griff Bilbro and W. L. McMillan, Phys. Rev. B **14**, 1887 (1976).

[6] K. Machida, J. Phys. Soc. Jpn. **50**, 2195 (1981).

[7] G. C. Psaltakis, J. Phys. C **17**, 2145 (1984).

[8] T. Vuletic, P. Auban-Senzier, C. Pasquier *et al.*, Eur. Phys. J. B **25**, 319 (2002).

[9] D. Andres, M. V. Kartsovnik, W. Biberacher, K. Neumaier, E. Schuberth, and H. Müller, Phys. Rev. B **72**, 174513 (2005).

[10] A. M. Clogston, Phys. Rev. Lett. **9**, 266 (1962); B. S. Chandrasekhar, Appl. Phys. Lett. **1**, 7 (1962).

[11] I. J. Lee, M. J. Naughton, G. M. Danner, and P. M. Chaikin, Phys. Rev. Lett. **78**, 3555 (1997); I. J. Lee, P. M. Chaikin, and M. J. Naughton, Phys. Rev. B **62**, R14669 (2000).

[12] I. J. Lee, P. M. Chaikin, and M. J. Naughton, Phys. Rev. B **65**, 180502(R) (2002).

[13] I. J. Lee, S. E. Brown, W. G. Clark, M. J. Strouse, M. J. Naughton, W. Kang, and P. M. Chaikin, Phys. Rev. Lett. **88**, 017004 (2001); I. J. Lee, D. S. Chow, W. G. Clark, M. J. Strouse, M. J. Naughton, P. M. Chaikin, and S. E. Brown, Phys. Rev. B **68**, 092510 (2003).

[14] I. J. Lee, P. M. Chaikin, and M. J. Naughton, Phys. Rev. Lett. **88**, 207002 (2002).

[15] I. J. Lee, S. E. Brown, W. Yu, M. J. Naughton, and P. M. Chaikin, Phys. Rev. Lett. **94**, 197001 (2005).

[16] L. P. Gor'kov and P. D. Grigorev, Europhys. Lett. **71**, 425 (2005).

[17] L. P. Gor'kov and P. D. Grigoriev, Phys. Rev. B **75**, 020507(R) (2007).

[18] S. A. Brazovskii and N. N. Kirova, Sov. Sci. Rev., Sect. A **5**, 99 (1984).

[19] W. P. Su and J. R. Schrieffer, in *Physics in One Dimension*, Springer Series in Solid State Sciences, edited by J. Bernascony and T. Schneider (Springer, New York, 1981).

[20] S. Brown (unpublished).

[21] The spin structure of SC state in the presence of SDW was also investigated in the model of Ref. 46, where the SC order parameter appears on both well-nested and bad-nested parts of the Fermi surface. Then such SC order parameter contains a mixture of spin-singlet and spin-triplet order parameters (Ref. 46). In this paper the model in Ref. 17 is considered, where the DW and SC order parameters are separated in the momentum or in the coordinate space.

[22] S. A. Brazovskii, L. P. Gor'kov, and A. G. Lebed', Zh. Eksp. Teor. Fiz. **83**, 1198 (1982) [Sov. Phys. JETP **56**, 683 (1982)]

[23] J. Bardeen, L. N. Cooper, and J. R. Schrieffer, Phys. Rev. **108**, 1175 (1957).

[24] J. Solyom, Adv. Phys. **28**, 201 (1979).

[25] N. Dupuis, C. Bourbonnais, and J. C. Nickel, Fiz. Nizk. Temp. **32**, 505 (2006).

[26] K. Kuroki, J. Phys. Soc. Jpn. **75**, 051013 (2006).

[27] Yu. A. Bychkov, L. P. Gor'kov, and I. E. Dzyaloshinskii, Zh. Eksp. Teor. Fiz. **50**, 738 (1966) [Sov. Phys. JETP **23**, 489 (1966)].

[28] Y. Tanaka and K. Kuroki, Phys. Rev. B **70**, 060502(R) (2004).

[29] M. T. Beal-Monod, C. Bourbonnais, and V. J. Emery, Phys. Rev. B **34**, 7716 (1986).

[30] J. C. Nickel, R. Duprat, C. Bourbonnais, and N. Dupuis, Phys. Rev. Lett. **95**, 247001 (2005).

[31] Y. Fuseya and Y. Suzumura, J. Phys. Soc. Jpn. **74**, 1263 (2005).

[32] T. Nomura and K. Yamada, J. Phys. Soc. Jpn. **70**, 2694 (2001).

[33] H. Kino and H. Kontani, J. Low Temp. Phys. **117**, 317 (1999).

[34] S. Belin and K. Behnia, Phys. Rev. Lett. **79**, 2125 (1997).

[35] The generalization of the mean-field description of DW in quasi-1D metals in the presence of magnetic field was elaborated in Ref. 48 for SDW and in Refs. 49 and 50 for CDW. A strong magnetic field, acting on CDW state, mixes the SDW and CDW order parameters (Refs. 49 and 50) and may lead to the series of phase transitions between the states with different quantized values of the nesting vector (Ref. 51). A strong magnetic field, acting on metals with imperfect nesting, can lead to the field-induced DW (Ref. 52).

[36] Usually, $\delta \propto P - P_{c1}$. However, the reduction in the energy gap Δ_0, accompanying the formation of ungapped pockets and the reduction in the nested part of FS, can make the growth $\delta(P)$ faster at $P = P_{c1}$.

[37] A. A. Abrikosov, L. P. Gor'kov, and I. E. Dzyaloshinskii, *Methods of Quantum Field Theory in Statistical Physics* (Dover, New York, 1977).

[38] A. M. Gabovich and A. S. Shpigel, Phys. Rev. B **38**, 297 (1988).

[39] Charles Ro and K. Levin, Phys. Rev. B **29**, 6155 (1984).

[40] Proposed in Ref. 47, the appearance of an additional spatially modulated SC order parameter $\Delta_{SC}(Q_N)$ seems to be negligible (or wrong) when the Fermi energy is much greater than the DW and SC order parameters.

[41] L. P. Gor'kov and T. K. Melik-Barkhudarov, Zh. Eksp. Teor. Fiz. **45**, 1493 (1963) [Sov. Phys. JETP **18**, 1031 (1963)].

[42] J. B. Ketterson and S. N. Song, *Superconductivity* (Cambridge University Press, Cambridge, 1999).

[43] A. E. Kovalev, S. Hill, and J. S. Qualls, Phys. Rev. B **66**, 134513 (2002).

[44] R. Kondo, S. Kagoshima, and M. Maesato, Phys. Rev. B **67**, 134519 (2003).

[45] L. P. Gor'kov and D. Jérome, J. Phys. (France) Lett. **46**, L643 (1985).

[46] G. C. Psaltakis and E. W. Fenton, J. Phys. C **16**, 3913 (1983).

[47] K. Machida, T. Kōnyama, and T. Matsubara, Phys. Rev. B **23**, 99 (1981).

[48] A. Bjeliš and D. Zanchi, Phys. Rev. B **49**, 5968 (1994).

[49] D. Zanchi, A. Bjeliš, and G. Montambaux, Phys. Rev. B **53**, 1240 (1996).

[50] P. D. Grigoriev and D. S. Lyubshin, Phys. Rev. B **72**, 195106 (2005).

[51] D. Andres, M. V. Kartsovnik, P. D. Grigoriev, W. Biberacher, and H. Müller, Phys. Rev. B **68**, 201101(R) (2003).

[52] L. P. Gor'kov and A. G. Lebed, J. Phys. (Paris) **45**, L433 (1984); G. Montambaux, M. Heritier, and P. Lederer, Phys. Rev. Lett. **55**, 2078 (1985); A. G. Lebed, *ibid.* **88**, 177001 (2002); Pis'ma Zh. Teor. Eksp. Fiz. **72**, 205 (2000) [JETP Lett. **72**, 141 (2000)].